ACS APPLIED MATERIALS & INTERFACES

Research Article

www.acsami.org

pH-Responsive One-Dimensional Periodic Relief Grating of Polymer Brush–Gold Nanoassemblies on Silicon Surface

Jem-Kun Chen,*[,†] Ping-Chun Pai,[†] Jia-Yaw Chang,[‡] and Shih-Kang Fan[§]

[†]Department of Materials Science and Engineering and [‡]Department of Chemical Enigneering, National Taiwan University of Science and Technology, 43, Sec 4, Keelung Rd, Taipei, 106, Taiwan, Republic of China

[§]Department of Materials Science and Engineering, National Chiao Tung University, 1001 University Road, Hsinchu, Taiwan 300, Republic of China

ABSTRACT: In this work, we focus on the fabrication of the nanoassemblies consisting of the poly(2-dimethylaminoethyl methacrylate) (PDMAEMA) brushes and gold nanoparticles (AuNPs). The employed process involves grafting of the PDMAEMA chains on an underlying substrate in a brush conformation followed by the immobilization of surface functionalized AuNPs by means of physical interaction (electrostatic attraction, entanglement, and hydrogen bonding). Atomic force microscopy (AFM), X-ray photoelectron spectroscopy (XPS), and UV–vis spectroscopy have been employed to characterize the prepared PDMAEMA-AuNP nanoassemblies. Polymer brushes possessing various thicknesses have been found to suppress the nanoparticles' aggregation and, hence, facilitate the surface coverage. Furthermore, we patterned the PDMAEMA-AuNP nanoassemblies as an one-dimensional periodic relief grating (OPRG). The subwavelength structure of OPRG has the optical features including artificial refractive index, form birefringence and resonance and band gap effects. A mean refractive index of the PDMAEMA-AuNP nanoassemblies can be controlled by the filling factors of the OPRG structure, so that a desired distribution of refractive index of the polymer brushes-gold OPRG under various stimuli can be realized. The employed approach is simple and highly versatile for the modification of surfaces with a wide range of NPs.

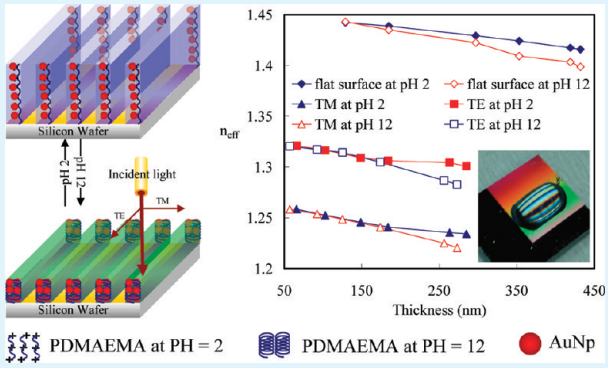

KEYWORDS: *PDMAEMA brush, nanolithography, gold nanoparticles, binary grating*

INTRODUCTION

Metal nanoparticles (NPs) represent a special class of the materials, which has recently attracted much attention of the researchers because of their fascinating properties and potential applications in a wide range of areas including in the fabrication of nanosensors, electronics and optical devices.[1] A great deal of the research efforts have been devoted to the gold (Au) NPs because of their unique properties.[2,3] In addition, many attempts have been made for the immobilization of AuNPs on macroscopic surfaces in order to improve the accessibility of their unusual optical properties. In comparison to the stabilization with gels or other 3D matrixes, one can access a relatively higher surface area of the NPs by means of their immobilization over macroscopic surfaces, as in the previous case NPs remain partly or wholly inside the gels.[4] Due to the high surface energy, they tend to aggregate, and aggregation limits their use in above-mentioned applications. A great deal of effort has been devoted to the stabilization of NPs by exploiting a wide range of stabilizers such as self-assembled monolayers,[5] polymer brushes,[6] block copolymers,[7] latex particles,[8] microgels,[9] and so on.[10] Among these systems, polymer brushes have been found to offer an easy and effective way for the stabilization of NPs on macroscopic surfaces. Stable polymer brushes can provide excellent mechanical and chemical protection to a substrate, alter the electrochemical characteristics of an interface, and provide new pathways for the functionalization of Si surfaces.[11,12] One particular advantage that polymer brushes have over spin-coated polymer layers is their stability against solvents, resulting from their covalent bonding to the substrates. In addition, polymer brushes are the assemblies of macromolecules that are tethered by one end to the underlined substrate in such a way that the distance between two grafted chains is lower than that of the radius of the gyration of a polymer chain.[12] Earlier studies demonstrate that polymer brushes serve as a perfect template for the preparation, stabilization, and application of NPs on the account of their nanometer dimensions, well-defined structure, and ability to control assembly of NPs over multiple length scales, superior precision over template architecture, and the availability of a greater variety of functional groups.[13,14]

Fabrication of ordered arrays of nanoparticles is of significance for both fundamental science associated with low-

Received: November 22, 2011
Accepted: March 16, 2012
Published: March 16, 2012

 © 2012 American Chemical Society

dimensional physics and technical applications.[15] The fabrication of well-defined chemical patterns, in terms of both chemistry and geometry, is critical for a number of important applications.[16] Perhaps two of the most demanding applications are the directed assembly of block copolymers[17,18] and the site-specific immobilization of NPs.[19] In the case of NP immobilization, chemical patterning of the surface has proven to be a highly promising strategy for the specific placement of NPs as it provides robust and controllable substrate particle interaction.[19,20] Chemical nanopatterns have typically been fabricated in two different ways to achieve site-specific NP placement. In one general approach, self-assembled monolayers (SAMs) are deposited on lithographically defined regions of a silicon substrate, and then AuNPs are immobilized to the SAMs via electrostatic attraction. For example, lines of amino-propyltriethoxysilane (APTES) were deposited on silicon oxide after patterning poly(methyl methacrylate) photoresist with electron beam lithography, and negatively charged AuNPs subsequently adhered to the APTES.[21] In similar work, lithographically patterned lines of Au on silicon oxide could be used to fabricate patterns of SAMs, comprised of either APTES[22] on silicon oxide or aminoterminated alkanethiols on Au,[20] and then AuNPs were selectively immobilized on the amino groups. The interest in these polymer brush−metal nanocomposite films is due to the unusual or new optical, catalytic, and mechanical properties that can be endowed by the metal nanoparticles in combination with the possibilities offered by the polymer brush to introduce responsiveness to external stimuli such as temperature or ionic strength.[23,24]

Polymer brush patterns designed for directed assembly of polymers often have been fabricated from a homogeneous thin organic film that was lithographically patterned and subsequently etched with an oxygen plasma to remove, either completely or partially, the film material in selected areas.[25,26] The initial film was formed from SAMs,[27] polymer brushes,[27,28] or polymer mats.[29] The chemistry of the guiding regions was dependent on the etching conditions, and the chemistry of the protected regions could also be affected by the lithographic and etch processes. The need for increasingly precise control of chemical pattern feature dimensions and chemistry has been highlighted by recent directed assembly results in which the assembled block copolymer feature density was an integral multiple of the chemical pattern feature density.[30,31] Herein, we report on an easy and facile approach to the immobilization of AuNPs on surfaces by exploiting chemically grafted and well-defined poly(2-dimethylaminoethyl methacrylate) (PDMAEMA) brushes as surface modifiers. In this process, the polymer brush has multiple functions: (i) it acts as a matrix that can be loaded with precursor ions; (ii) it allows the immobilization of the resulting nanoparticles and prevents their aggregation and (iii) it serves as a capping agent to limit nanoparticle growth. The modified AuNPs and PDMAEMA are good donor and acceptor in hydrogen bonding system, respectively, to generate electrostatic interaction among them.[32,33] We speculate that the electrostatic attraction of tertiary amine groups and hydrogen bonding between carboxyl groups of PDMAEMA chains present at the surface of AuNPs acts as the driving force for fabrication of these nanoassemblies (scheme 1). Furthermore, the employed protocol involves grafting of PDMAEMA chains on an underlined substrate as one-dimensional periodic relief grating (OPRG) in brush conformation followed by immobilization of the preformed and carboxyl-functionalized AuNPs on the patterned PDMAEMA brushes. We first fabricate

Scheme 1. Hydrogen Bonding between Tertiary Amine Groups of PDMAEMA Chains and Carboxyl Groups Present at the Surface of AuNPs Acts As the Driving Force for Fabrication of These Nanoassemblies

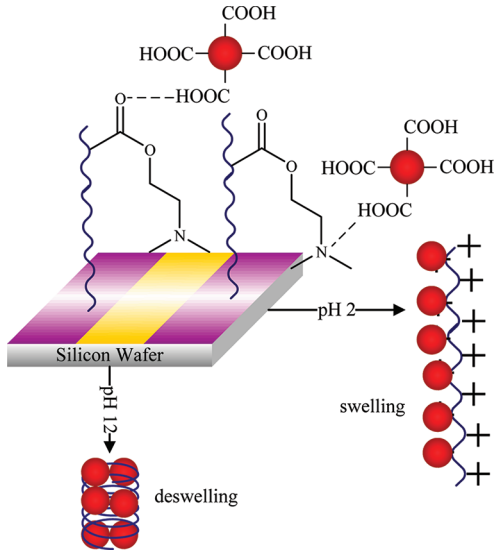

polymer brushes-gold nanoassemblies as an OPRG. The subwavelength structure of OPRG has the optical features including artificial refractive index, form birefringence and resonance and band gap effects. A mean refractive index of the polymer brushes-gold nanoassemblies can be controlled by the filling factors of the OPRG structure, so that a desired distribution of refractive index of the polymer brushes-gold OPRG under various stimuli can be realized. In addition, the OPRG structure causes optically anisotropy called form birefringence. When the grating period is in the order of the light wavelength, the light wave may resonate and be reflected in the structure, so that resonant reflection occurs. These optical features produce new optical elements of the polymer brushes-gold nanoassemblies for sensor application. Employed approach resulted into a homogeneous, dense, and completely covered surface of PDMAENA-AuNPs OPRG. External stimuli induced modulation in the filling factor of PDMAENA-AuNPs OPRG affords great opportunities for a wide range of nanotechnological areas and opens up a new avenue on the account of tunable optical properties in nanosensor applications.

EXPERIMENTAL SECTION

Materials. Highly polished on one side (diameter: 6 in.) single-crystal silicon wafers of (100) orientation with ca. 1.5 nm thick native silicon oxide layers were purchased from Hitachi, Inc. (Japan) and cut into 2 cm ×2 cm samples as substrates. The materials used for graft polymerization, 3-aminopropyltriethoxysilane (AS) and 2-bromo-2-methylpropionyl bromide (BB), 2-bimethylaminoethyl methacrylate, copper(I) bromide, copper(II) bromide, triethylamine (TA), and 1,1,4,7,7-pentamethyldiethylenetriamin (PMDETA), were purchased from Acros Organics Co. DMAEMA, PMDETA, AS and BB were purified through vacuum distillation prior to use. The materials used for AuNP synthesis, hydrogen tetrachloroaurate(III) trihydrate ($HAuCl_4$), tetra-n-octylammonium bromide (TOAB; $C_{32}H_{38}BrN$), mercaptoacetic acid (MAA), and sodium borohydride ($NaBH_4$), were purchased from Acros Organics. All other chemicals and solvents were of reagent grade and purchased from Aldrich Chemical Co and used without additional purification. To remove dust particles and organic contaminants, the Si surfaces were ultrasonically rinsed sequentially

with methanol, acetone, and dichloromethane for 10 min each and subsequently dried under vacuum. The Si substrates were immersed in hydrofluoric acid solution (50 wt %) for 5 min at room temperature to remove the silicon oxide film. The hydrofluoric acid-treated substrates were then immersed in the mixture of H_2SO_4 and H_2O_2 (2:1, mol %) for 5 min and subsequently rinsed with doubly distilled water a minimum of five times to oxidize the Si. To stabilize the ionic strength, the deionic water was used as a buffer solution in this work.

Preparation of Patterned Polymer Brushes as Line Array. The basic strategy for the fabrication of the patterned polymer brushes as line array using the very-large-scale integration (VLSI) process has been described previously.[34] The fabrication process is depicted as shown in Figure 1. A: The Si wafer was treated with hexamethyldisilazane (HMDS) in a thermal evaporator (Track MK-8) at 90 °C for 30 s to transform the OH groups on the surface of the wafer into an inert film of $Si(CH_3)_3$ groups. The photoresist was spun on the HMDS-treated Si wafer at a thickness of 690 nm. E-beam lithography was then used to pattern the photoresist with an array of 400 nm resolution trenches after development. B: The sample was then subjected to oxygen plasma treatment (OPT) using a TCP 9400SE instrument (Lam Research Co, Ltd.) to form OH groups from the HMDS-treated surface. OPT caused the surface to become chemically modified (strongly hydrophilic or polar) only in the areas not covered by the photoresist.[34,35] The introduction of these polar groups provided a more wettable surface for the preparation of a SAM for graft polymerization. The remaining photoresist was removed from the HMDS-treated surface by rinsing with solvent, leaving behind the chemically nanopatterned surface. C: To immobilize the ATRP initiator, the Si substrate treated with HMDS and OPT was immersed in a 0.5% (w/v) solution of AS in toluene for 2 h at 50 °C. The AS units assembled selectively onto the bare regions of the Si surface after OPT, where it reacted with Si−O and Si−O−O species. D: Sequentially, the sample was immersed in both of 2% (v/v) solution of BB and TA in tetrahydrofuran (THF) for 8 h at 20 °C. After reaction, the wafers were placed in a Soxhlet apparatus to remove any nongrafted material. This procedure resulted in a surface patterned with regions of AS-BB for ATRP and regions of HMDS. The functionalized Si substrates were removed from the solution, washed with toluene for 15 min to remove any unreacted material, dried under a stream of nitrogen, and subjected to surface-initiated polymerization reactions. Finally, the surfaces were dried under a vacuum and stored under a dry N_2 atmosphere. E: The patterned PDMAEMA brushes were grafted on the initiator-modified Si surface by ATRP. For the preparation of PDMAEMA brushes on the Si-AS-BB surface, DMAEMA, Cu(I)Br, $CuBr_2$, and PMDETA were added to dimethylformamide (DMF), extra-dry DMF. The solution was stirred and deoxygenated with Ar for 15 min at 90 °C. The Si-AS-BB substrate was then added to the solution. After various polymerization times, the wafers were placed in a Soxhlet apparatus to remove any unreacted monomer, catalyst, and nongrafted material. The surfaces were then dried under vacuum at 80 °C for 20 min. The polymer-modified Si surfaces were analyzed using ellipsometry (SOPRA SE-5, France) and X-ray photoelectron spectroscopy (XPS; Scientific Theta Probe, UK). In addition, samples of "free" PDMAEMA were synthesized in solution under the same conditions ([DMAEMA]:[BB]:[CuBr]:[PMDETA] = 300:1:1:1; [DMAEMA] = 2.0 M) as those used for grafting polymerization to provide polymers having the same molecular weights of PDMAEMA as the brushes grafted on the Si surface. The "free" PDMAEMA generated in solution from the sacrificial initiator was recovered through precipitation of the reaction mixture into cyclohexane; it was analyzed using ^1H nuclear magnetic resonance (NMR; BRUKER AVANCE 500) instrument as shown in Figure 2.[36] The monomer conversion was determined gravimetrically. Gel permeation chromatography (GPC) measurements were performed using a VISCOTEK-DM400 instrument equipped with an LR 40 refractive index detector. The resolutions of the various line patterns of PDMAEMA brushes were measured using atomic force microscopy (AFM; Veeco Dimension 5000 scanning probe microscope) and high-resolution scanning electron microscopy (HR-SEM;

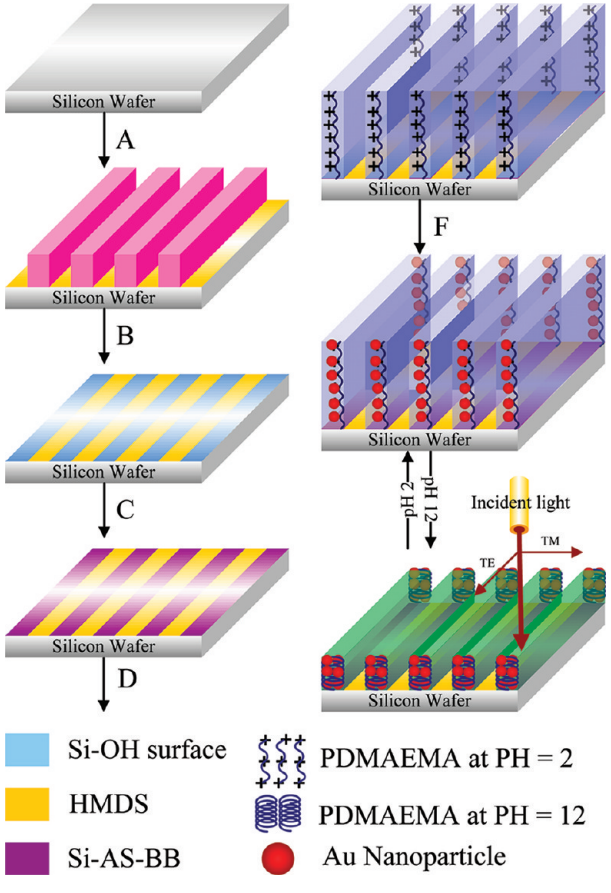

Figure 1. Schematic representation of the immobilization of AuNPs on OPRG of pH-responsive PDMAEMA brushes on a surface. (A) Si wafer treated with HMDS in a thermal evaporator. Photoresist spin-coated onto the Si surface presenting $Si(CH_3)_3$ groups. E-beam lithography used to pattern the photoresist with arrays of trenches on the surface. (B) OPT used to chemically modify the exposed regions presenting $Si(OCH_3)_3$ groups and to convert the topographic photoresist pattern into a chemical surface pattern. Photoresist removed through treatment with solvent. (C) AS selectively assembled onto regions of the OPT-treated Si surface. BB selectively reacted with AS-treated Si surface to form the initiator. (E) Sample grafting via surface-initiated ATRP of DMAEMA from the functionalized areas of the patterned SAM as OPRG. (F) Immobilization of AuNPs on the OPRG of pH-responsive polymer brushes by electrostatic attraction and hydrogen bonding exhibits pH-dependent behavior on optical property from pH 2 and 12.

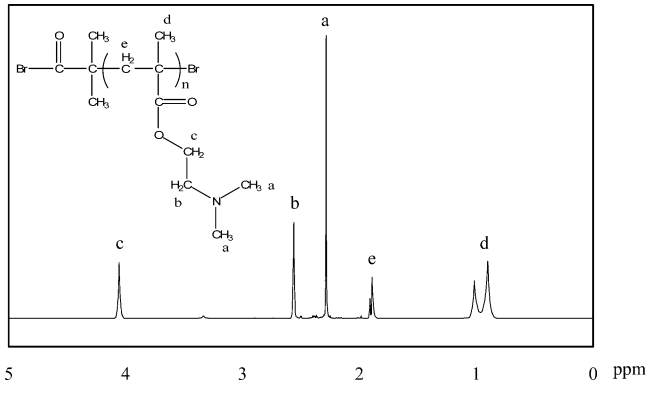

Figure 2. ^1H NMR spectrum of "free" PDMAEMA polymerized by ATRP with BB as an initiator.

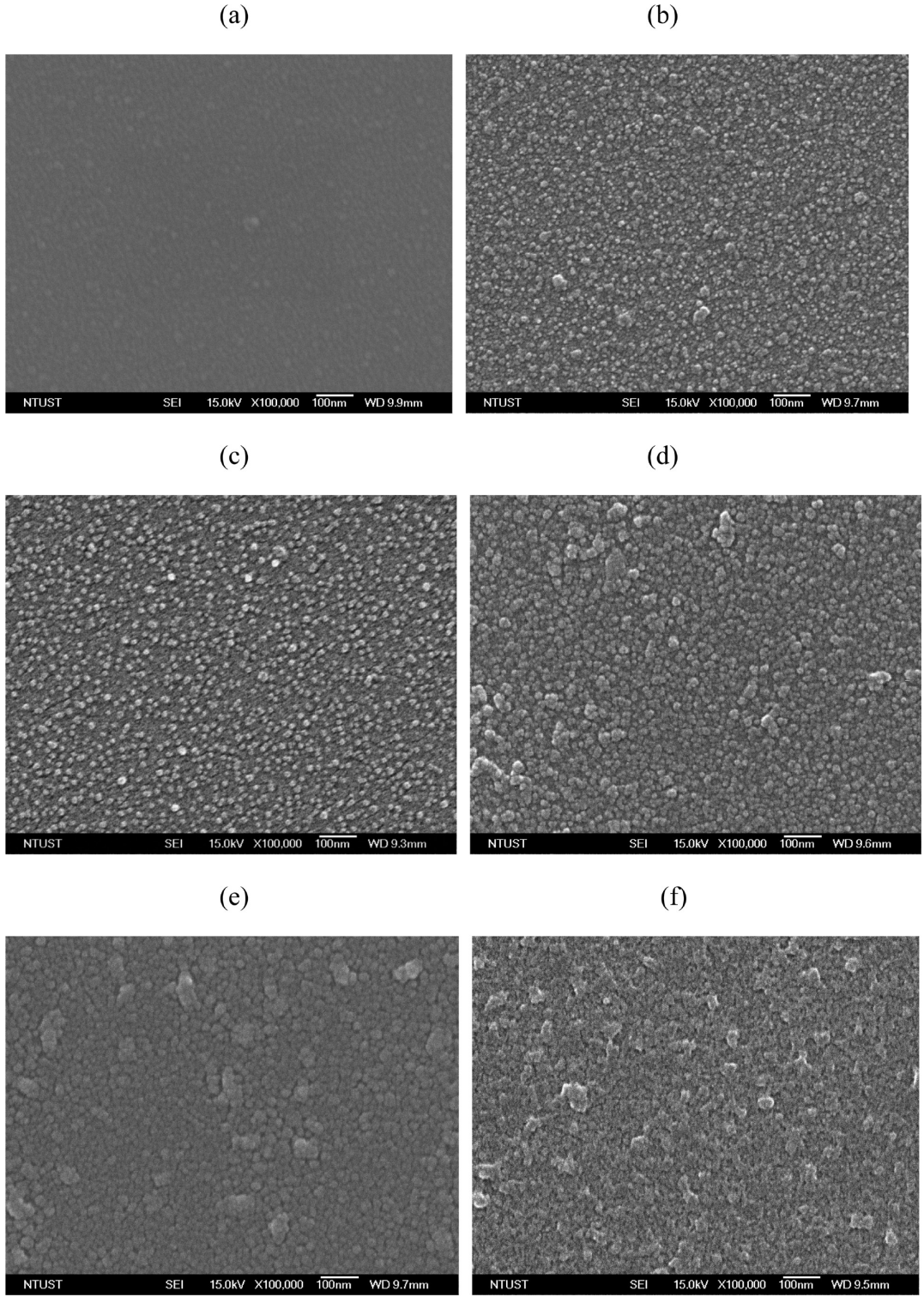

Figure 3. Topographic SEM images of the (a) Si–AS-BB surface, and Si–PDMAEMA surfaces obtained after (b) 2, (c) 4, (d) 8, (e) 16, and (f) 24 h of grafting time.

JEOL JSM-6500F, Japan). To observe the AuNP distribution on PDMAEMA brushes at pH 2 and 12, the Si-PDMAEMA samples possessing various thicknesses are prepared by their overnight incubation at pH 2 and 12. Sequentially, the subjects were treated under −40 °C for 10 min to remove the water in vacuum freeze-dryer (BENCHTOP 2K; VIRTIS; America).

Immobilization of AuNPs on PDMAEMA Brushes. AuNPs were synthesized by borohydride reduction of chlorauric acid as described elsewhere.[37] In a typical process, 50 mL of aqueous solution of $HAuCl_4 \cdot 4H_2O$ was mixed with TOAB dissolved in 100 mL of toluene, and subsequently, the resulting mixture was added to a solution of MAA in 25 mL of toluene dropwise under vigorous stirring at room temperature. A freshly prepared 25 mL aqueous solution of $NaBH_4$ was added into the reaction media, and the resulting mixture was allowed to stir for another 1 h. The colloidal solutions obtained were very stable and did not show signs of decomposition or aggregation over a period of several weeks. The specimens for examination by electron microscopy were prepared by evaporation of

Table 1. Characterization of Grafted PDMAEMA Brushes on Silicon Surface by ATRP

grafting time (hr)	M_n (mol/g)	PDI	dry thickness (nm)	Re (nm)	σ (chain/nm^2)	roughness (nm)	Sc[a] (g/m^2)	WCA (degree)	zeta potential (mV)
2	13 299	1.10	129 ± 5	0.36	7.58	2.189	0.17	54.7 ± 4	−34.6 ± 5
4	22 249	1.22	185 ± 7	0.40	6.36	1.571	0.24	55.1 ± 4	−30.8 ± 3
6	28 272	1.07	297 ± 6	0.35	8.21	1.124	0.39	49.7 ± 4	−25.4 ± 4
8	32 326	1.16	353 ± 5	0.34	8.87	0.817	0.48	48.3 ± 3	−23.5 ± 3
16	38 958	1.13	419 ± 4	0.34	8.51	0.817	0.55	48.9 ± 3	−21.9 ± 3
24	40 319	1.23	432 ± 4	0.34	8.47	2.189	0.17	48.6 ± 3	−20.5 ± 2

[a]Surface coverage (Sc) = film thickness × density.

one or two drops of a toluene solution of the nanoparticles on to holey carbon films supported on standard copper grids. The UV−vis spectrum of the gold solution was similar to that obtained by lambda 25 spectrophotometer (Perkin-Elmer) for gold hydrosols of 5−6 nm average particle diameter. Finally, AuNPs were immobilized on PDMAEMA brushes modified silicon substrates by incubating the samples into their 1 mM solution in toluene, overnight. Non- or weakly adsorbed particles were removed by repetitive rinsing of the samples with toluene. The thicknesses of the grafted polymer brushes were measured at λ = 633 nm and an incidence angle of 75° with a scanning ellipsometry equipped with an XY-positioning table for mapping of the sample surface. The measurements were performed for each sample after each step of the modification to use the measurements of the previous step as a reference for the simulation of ellipsometric data.[38] The refractive indices for the calculations were 3.858, 1.4598, 1.513, and 0.179 for silicon substrate, native silica layer, PDMAEMA brushes, and Au at 633 nm, respectively.

pH-Responsive OPRG of PDMAEMA-AuNP Nanoassemblies. Supposing multi1ayered thin film stacks as a one-dimensional periodic structure, the wavenumber of the eigenmode in the stacks can be expressed by a simple closed form equation.[39] The effective refractive indices can be obtained by solving the simple nonlinear equation. Especially when the structure period is shorter than the light wavelength, the above closed form equation is assumed to be a very simple equation, consequently the structure is equivalent to a negative uniaxial anisotropic optical crystal. In this case, the optical axis is perpendicular to the stacked films, and the effective refractive index of the ordinary wave $n_{||}$ is expressed by

$$n_{\|}^2 = (1 - f)n_1^2 + fn_2^2 \quad (4)$$

where f is the filling factor of the material of n_2. This equation means that the average of dielectric constants corresponds to the effective dielectric constant. For the extraordinary wave the effective index $n_\perp$ is

$$\frac{1}{n_\perp^2} = \frac{1 - f}{n_1^2} + \frac{f}{n_2^2} \quad (5)$$

In case of a one-dimensional binary relief grating as shown in Figure 1, the effective refractive index for TE polarization is $n_{||}$, and the index for TM polarization is $n_\perp$. The effective refractive indices of pH-responsive polymer-modified Si surfaces were obtained using ellipsometry.

RESULTS AND DISCUSSION

Characterization of PDMAEMA Brushes. Well-defined and homogenously distributed PDMAEMA brushes were prepared on a silicon substrate by exploiting the well-known "grafting from" approach.[40] It is well-known from literature that our various stages can be used as a universal anchoring layer for grafting of a variety of polymer brushes on a silicon substrate. The chemical compositions of the pristine Si(100) surface and the Si surfaces at various stages during the surface modification process were determined using XPS in pervious study.[41] Figure 3a presents representative SEM images of the Si-AS-BB surface. The AS-BB layer generates a SAM layer of grafted sites on the surface. Figure 3b−f display SEM images of the morphologies of the PDMAEMA brushes grafted onto the Si surfaces via ATRP for 2, 4, 8, 16, and 24 h, respectively. Obvious clusters of tethered PDMAEMA possessing particle sizes from 19 to 36 nm formed from the grafted sites for 2, 4, and 8 h of grafting time, respectively (Figure 3b−d). The tethered PDMAEMA films were stacked with cluster particles for 16, and 24 h of grafting time to generate a thin film structure gradually on the surface. (Figure 3e,f) Grafting density of the PDMAEMA brushes has been estimated by $\sigma = 1/R_e^2$. Here, R_e is the root-mean-square end-to-end distance between two grafting sites which was derived from $R_e = M_n^{1/2}(N_A d\rho)^{-1/2}$, where M_n is number average molecular weight of polymer chains, N_A is Avogadro's number, ρ is polymer density for PDMAEMA (~1.318 g/cm^3), and d is dry state thickness of PDMAEMA brushes.[42] Table 1 summarizes the characterization of the PDMAEMA brushes for various grafting times onto the Si-AS-BB surfaces. The grafted PDMAEMA brushes on silicon surface by ATRP were negatively charged because of the residual negative electrostatic charges in the zeta potential instrument. The 185, 353, and 432 nm-thickness PDMAEMA brushes at pH 2 (left) and 12 (right) after lyophilizing were analyzed by SEM as shown in Figure 4a−c, respectively. At pH 2, the PDMAEMA brushes generate a dense layer on the surface with several bulges. Clusters appear gradually with the thickness of PDMAEMA brushes at pH 12. The observation corresponds to our previous reports about analysis of the pure PDMAEMA brushes grafted on the silicon surface via ATRP by AFM after incubation at various pH.[24,43]

Immobilization of AuNPs on PDMAEMA Brushes. Sequentially, the immobilization of AuNPs on polymer brushes has been realized by exploiting the physical interaction (electrostatic attraction and hydrogen bonding) between tertiary amine functionalities of PDMAEMA chains and surface functionalities (−COOH groups) of AuNPs that have been synthesized and modified with a shell of MAA as described.[44] TEM images of the AuNPs reveal their particle size in the range of 5 to 6 nm.[2] This fine dispersion of the AuNPs into the incubated aqueous solution results into their homogeneous distribution onto the PDMAEMA brushes.(Figure 5) Obtained PDMAEMA brushes-AuNP nanoassemblies have been thoroughly characterized with a variety of analytical tools after lyophilizing. Samples were cleaned with deionic water before lyophilizing them to ensure the complete removal of the nonimmobilized AuNPs. Figure 5a−c displays topographic SEM images of PDMAEMA brushes possessing 185, 353, and 432 nm thicknesses with the immobilization of AuNPs at pH 2 (left) and 12 (right). Comparing with the Figure 4, one can observe that the AuNPs appeared apparently on the thin film increase densely with the PDMAEMA thickness at pH 2.[45] The morphology has turned from "carpeted one" to "pebblelike" after tuning pH from 2 to 12, indicating that the AuNPs immobilized on the PDMAEMA brush toughly without disassembling during the change of the ionic strength in the

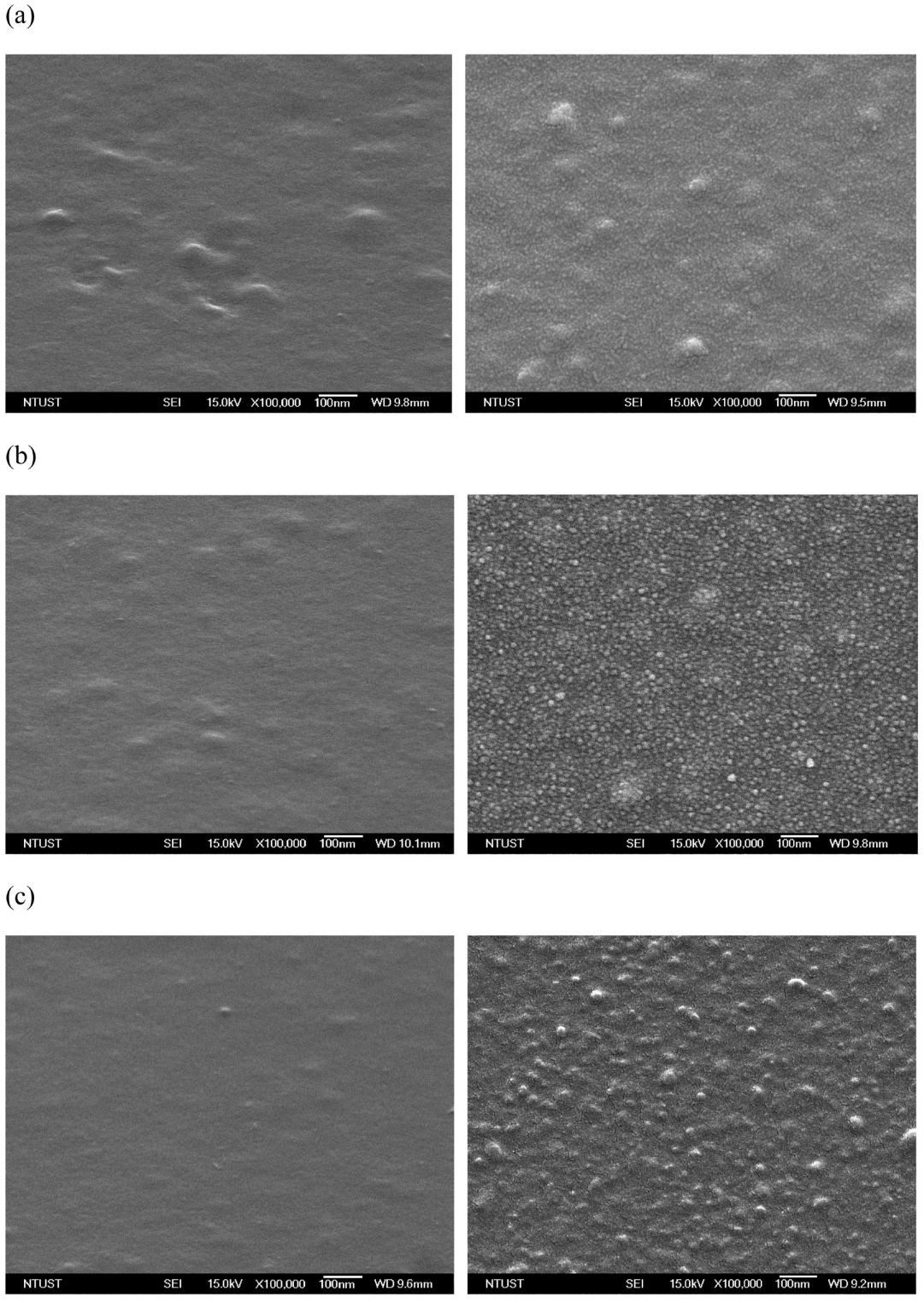

Figure 4. Topographic SEM images of bare PDMAEMA brushes possessing (a) 185, (b) 353, and (c) 432 nm of thickness at pH 2 (left) and 12 (right).

solution. The results may be explained by the entanglement between PDMAEMA and modified AuNPs. The pebble-like structure was analyzed specially by EDX of SEM, strongly confirming the presence of clusters of AuNPs onto the PDMAEMA brushes. The density of the pebble-like structure increased gradually with the thickness of tethered PDMAEMA due to the excessive positive charges promotion. (Figure 5a−c) Because the AuNPs immobilized at the upper part of PDMAEMA brushes, the numbers of AuNPs in a PDMAEMA domain estimated roughly through the spherical clusters in topographic SEM images at pH 12 gradually increase from ca. 12 to 33 nm with brush thickness. Moreover, the ionic strength has a strong effect on the interaction between the PDMAEMA brushes and AuNPs, but the nanoparticles disassembly from the brushes did not occur entirely when the pH was tuned from 2 to 12 to cause a strong repulsive force positively and negatively

dx.doi.org/10.1021/am201632e | *ACS Appl. Mater. Interfaces* 2012, 4, 1935−1947

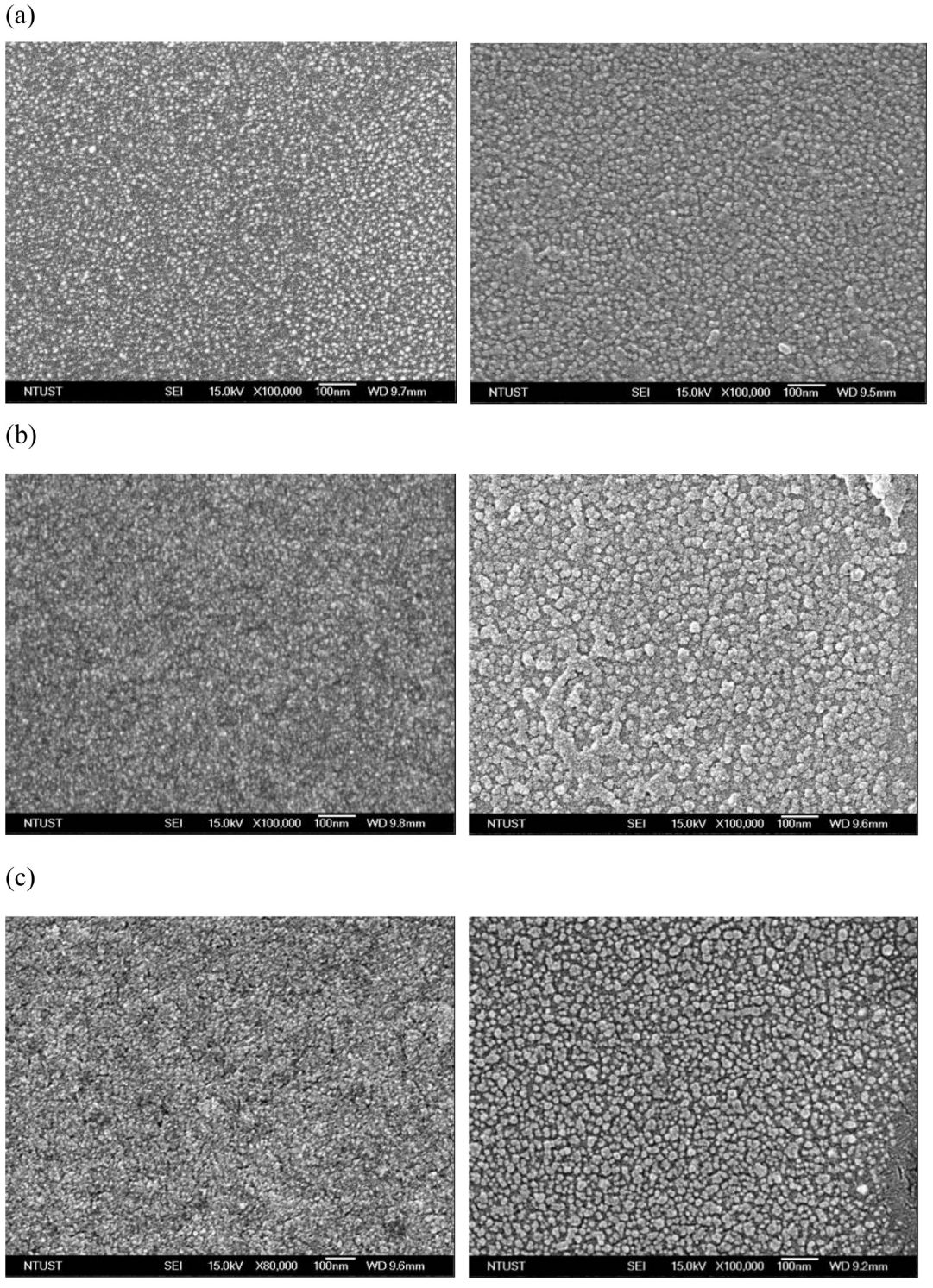

Figure 5. Topographic SEM images of AuNP immobilization on PDMAEMA brushes possessing (a) 185, (b) 353, and (c) 432 nm of thickness at pH 2 (left) and 12 (right).

charged among them. It may explain by the entanglement among the polymer chains and carboxyl groups during the hydrogen bonding and electrostatic attracting to stabilize partially the AuNPs on polymer layer. In order to rule out the fact that pH-responsive morphology of PDMAEMA-AuNP nanoassemblies after the pH-tuning process, the nanoassemblies have been incubated at pH 2 and 12 overnight and analyzed by AFM. A comparison of the phase (left) and height (right) AFM images of the nanoassemblies at pH 2 and 12 is used to distinguish from the variety in Figure 6. Figure 6a and 6d clearly reveal homogeneous PDMAEMA brushes possessing 185 and 432 nm of thicknesses without AuNP immobilization, respectively. It can be concluded that apparent pebbled structures in images b and e in Figure 6 are the sites of AuNPs at pH 2. It is also note worthy that the nanopatterns formed by PDMAEMA-AuNP nanoassemblies are spherical in shape and form a homogeneously distributed and closely packed layer at pH 2 on the surfaces. Figure 6c and 6f display

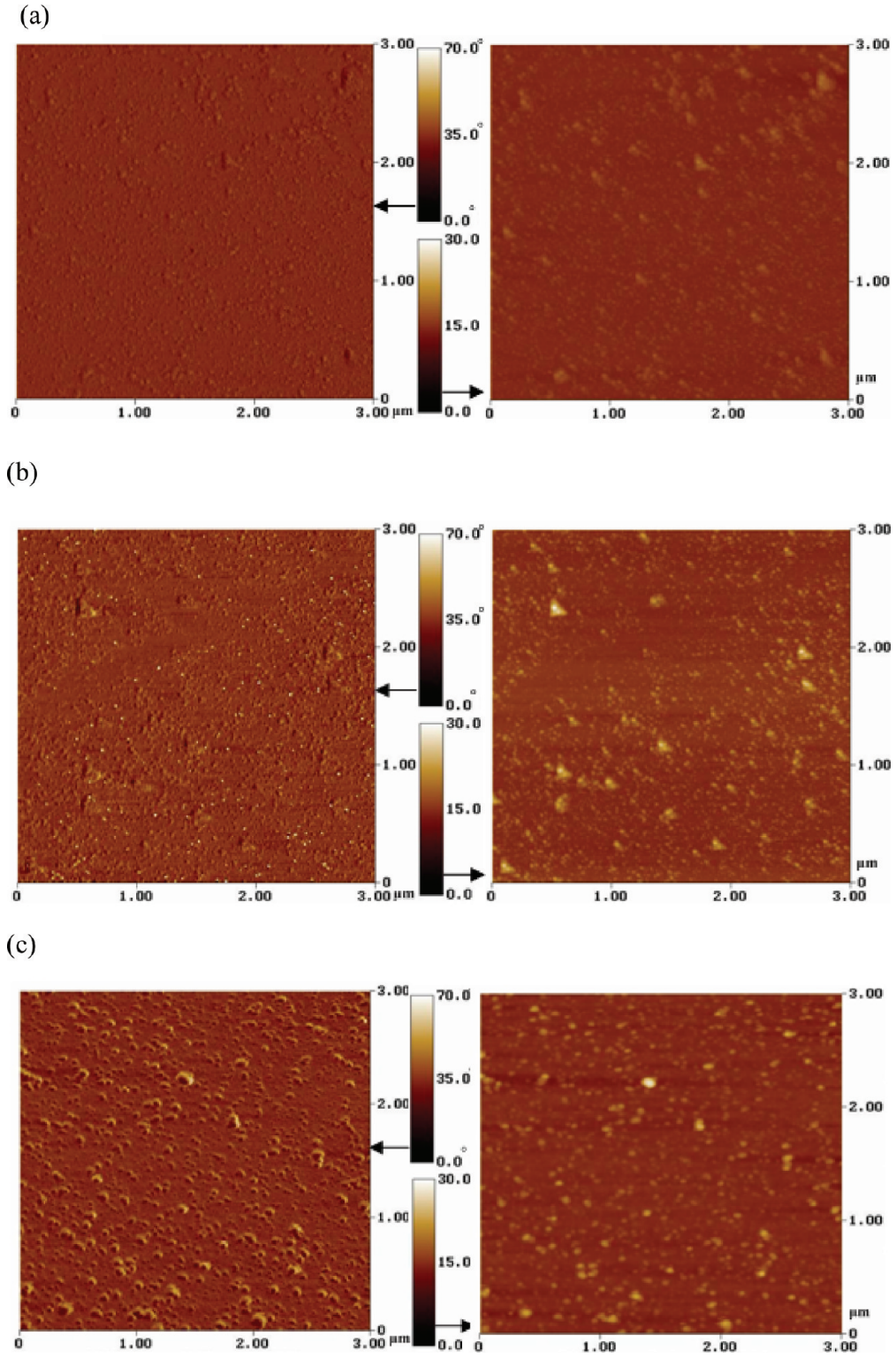

Figure 6. AFM phase (left) and height (right) images (3 × 3 μm) of PDMAEMA brushes with 185 nm (a) before and (b, c) after immobilization of AuNPs at (b) pH 2 and (c) 12, and PDMAEMA brushes with 432 nm (d) before and (e, f) after immobilization of AuNPs at (e) pH 2 and (f) 12.

the subjects after the immobilization of AuNPs at pH 12. The irregularly aggregated pebbles on the surface indicate the AuNP clustered on PDMAEMA brushes, indicating that the deswelling behavior of the PDMAEMA occurred at pH 12. Surface coverage (Φ) of AuNPs on polymer brushes was estimated by $\Phi = 100\% N\pi d^2/4A$, where d is the diameter of the nanocrystals and N is the number of AuNPs detected per area A.[11,42] The number of AuNPs per area of the sample was counted by zooming a part of the AFM, SEM images, and EDX analysis. A close inspection of these AFM images reveals that the described protocol is able to offer a homogeneous immobilization of AuNPs on macroscopic surfaces. Figure 7 presents dependence of thickness of the tethered PDMAEMA in terms of surface coverage of AuNPs on the polymer brushes.

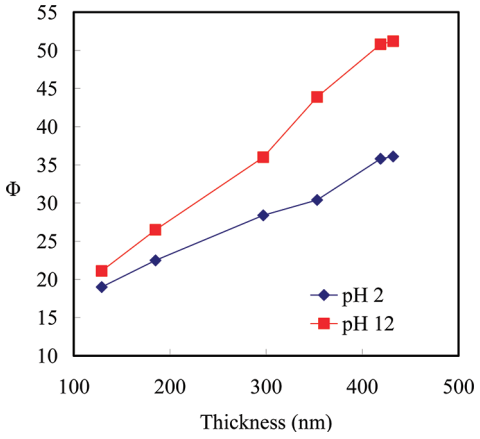

Figure 7. Surface coverage of AuNPs on PDMAEMA brushes (determined from SEM images) plotted as a function of the thickness.

For the flat substrate, a tethered PDMAEMA-AuNP nanoassemblies on the surface exhibited pH-dependent behavior at pH 2 and 12, respectively. The surface coverage increases substantially upon increasing thickness due to excessive positive charges promotion. At pH 2, the lower surface coverage attributes dispersed AuNPs inside the polymer brushes. At pH 12, the PDMAEMA-AuNP layer underwent excessive positive charges weakening, resulting in a compact and collapsed conformation of PDMAEMA chains to aggregate the AuNPs. Furthermore, the surface coverage of AuNP on the 432 nm-thickness polymer brushes approaches to 36.1% at pH 2; it returned to 51.2% after tuning pH from 2 to 12. For the432 nm thickness PDMAEMA brushes, this behavior was reversible for several cycles. These results suggest that the pH-responsive switching is related to the degree of excessive positive charges of the polymer brushes. The preparation of thin films with a high density of metal NPs is often desired for catalysis and electronics applications. It can be further evidenced by a significant change in root-mean-square (rms) roughness of brushes from 3.4 to 12.2 nm from pH 2 to 12. The presence of AuNPs on polymer brushes has been further evidenced by XPS analysis. Figure 8a shows a wide scan spectrum of PDMAEMA brushes immobilized with AuNPs. A comparison of this spectrum with that of bare PDMAEMA brushes reveals presence of the characteristic "Au" signals at relevant binding energies.[43] In addition, the inset in Figure 8b represents the XPS signature of the Au 4f doublet for the PDMAEMA-AuNPs brushes. The binding energies of the doublet for Au $4f_{7/2}$ and $4f_{5/2}$ have been found as 83.7 and 87.5 eV, respectively, which are consistent with the Au^0 oxidation state. In addition, it should also be noted that absence of a peak near 84.9 eV rules out the presence of any features due to the Au^+ oxidation state.[45] The atomic concentration of the Au on the investigated substrates has been found a linear approximately increases from 2.2% to 3.47% in thickness from 185 to 353 nm by XPS analysis. The atomic concentration of the Au reached a plateau on the polymer brush thickness from 353 to 432 nm indicates that most of the NPs are immobilized on the upper part of the polymer brushes. Because of the steric hindrance caused by the polymer chains, particles do not penetrate significantly into the longer brush layer.[11] In Figure 8c, the S 2p peak was observed in the spectrum of thiol-terminated surface of the PDMAEMA-AuNPs assembly. The S 2p peak could be resolved into three components of binding energies of 162, 164, and 165 eV which are assigned to thiolates (Au−S−) and unbound thiols

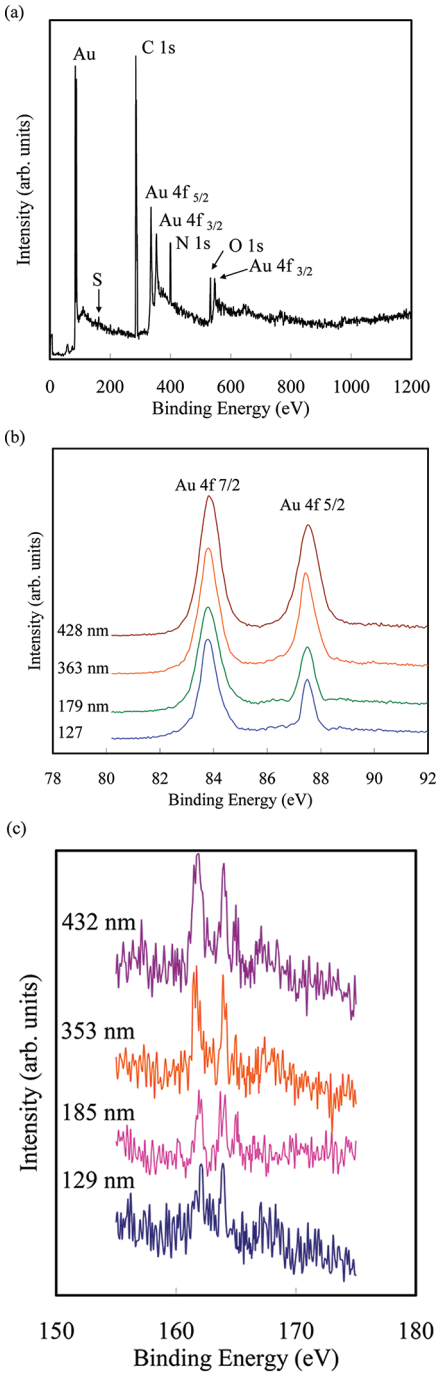

Figure 8. (a)XPS wide-scan spectrum of PDMAEMA brushes immobilized with AuNPs. (b) Au 4f and (c) S 2p core level spectra of the sample possessing various thicknesses.

(−SH−) (with S $2p_{3/2}$ and S $2p_{1/2}$ components), respectively.[46] The free thiols are attributed to the free end of MAA. Consequently, it is suggested that the gold−thiol bond does not have the character of gold sulfide. We summarized the chemical compositions of PDMAEMA and PDMAEMA −AuNP assemblies obtained from XPS in Table 2.[43]

It is well-known from the literature that modulation in size and proximity of the AuNPs leads to the shift in their surface plasmon resonance (SPR) band position. To achieve this variation in optical properties for nanosensor applications, AuNPs should be less than 20 nm in diameter with a narrow

dx.doi.org/10.1021/am201632e | ACS Appl. Mater. Interfaces 2012, 4, 1935−1947

Table 2. Chemical Composition of Si-PDMAEMA and Si-PDMAEMA-AuNP Nanoassemblies

	chemical composition of Si-PDMAEMA				chemical composition of Si-PDMAEMA-AuNP						
grafting time (h)	C 1s	O 1s	Si 2p	N 1s	C 1s	O 1s	Si 2p	N 1s	Au 4f	[Au/C][b]	film thickness (± 1.5 nm)
2	53.72	26.35	15.18	4.75	51.1	27.24	8.67	10.79	2.2	4.31	129
4	53.84	27.51	12.39	6.26	54.5	28.2	8.21	6.28	2.81	5.16	185
6	54.8	27.5	9.97	7.73	56.06	27.97	8.43	4.07	3.47	6.19	297
8	60.83	24.56	6.11	8.5	57.53	28.84	7.02	2.43	4.18	7.27	353
16	66.06	20.7	3.72	9.52	59.93	27.24	7.82	0.79	4.22	7.04	419
24	70.01	19.52	0.68	9.79	61.77	26.44	7.32	0.33	4.14	6.70	432

[a]Determined from XPS core level spectral area ratio. [b]Determined from the XPS curve-fitted C 1s and Au 4f core level spectra.

particle size distribution.[47] To investigate the optical properties of the free AuNPs and nanopatterns formed by polymer brushes with AuNPs at pH 2 and 12, samples have been analyzed by UV−vis spectroscopy and results are shown in Figure 9a. These free AuNPs indicate a strong SPR band at the characteristic position 520 nm. In addition, a symmetric absorption band at 554 nm for the AuNP immobilized on 432 nm -thickness PDMAEMA brushes in a dry state (purple curve) suggests the presence of AuNPs on the polymer brushes.[48,49] It is worth mentioning here that absence of the optical signature at a higher wavelength (>600 nm) excludes the possibilities of significant aggregation of immobilized AuNPs on the PDMAEMA brushes.[50] It has been realized that external stimuli induced modulation in the thickness of polymer brushes affords great opportunities for a wide range of nanotechnological areas and opens up a new avenue in nanosensor applications.[11] We investigated modulation in optical properties of AuNPs immobilized on PDMAEMA brushes with the variation in pH from air to water.(Figure 9a) One can observe that the SPR peak of PDMAEMA-AuNP nanoassemblies has shifted from 554 nm in the dry state (purple curve) to 531 nm in aqueous media at pH 2 (blue curve). With increasing pH to 12, the SPR peak of PDMAEMA-AuNP nanoassemblies has shifted from 531 nm at pH 2 to 542 nm in aqueous media at pH 12 (red curve). In addition, the absorption band of PDMAEMA-AuNPs in air has been found to be significantly broader than the one at pH 2. These observations can be attributed to the fact that PDMAEMA brushes swell in deionic water at pH 2 leading to the increase in interparticle distance among PDMAEMA-AuNP nanoassemblies. It is well-known from literature that an increase in interparticle distance of optically active NPs leads to the blue shift in their peak positions.[51] On the other hand, particles are relatively closer in the dry state as PDMAEMA chains are collapsed and a red shift in band position is observed. It should be noted that modulation in absorption band positions with the variation in surrounding media has been found nearly reversible. Underlying the swelling−deswelling behavior of PDMAEMA, we also examined the variation in optical properties of PDMAEMA-AuNP brushes at pH 2 and 12 in aqueous media. When samples have been immersed into the deionic water at pH 12, the SPR peak has been observed to red shift from 531 nm (blue curve in Figure 9a) to 542 nm (red curve in Figure 9a). In addition, the peak area has also been found to slightly increase, indicating the agglomeration of PDMAEMA-AuNP nanoassemblies with a decrease in pH. A schematic presentation of the swelling−deswelling behavior of polymer brushes with the change in pH and respective variation in peak position of PDMAEMA-AuNP nanoassemblies are shown in Scheme 1. This modulation in optical properties of AuNPs can be attributed to the pH induced collapse of PDMAEMA brushes at pH 12. As illustrated in Scheme 1, PDMAEMA chains include excessive positive charges promotion by means of electrostatic repulsion between polymer chains at pH 2 and, hence, remain in the swollen state. As the pH is increased above pH 12, they collapse without electrostatic repulsion. A decrease in interparticle distance caused by the collapse of polymer chains led to the red shift in the SPR peak. A comparison of the UV−vis spectrum of PDMAEMA-AuNP nanoassembly in the dry state with the one taken in the collapsed state in water at pH 12 reveals that AuNPs are closer in the previous case as compared to the later one. It can be attributed to the relatively higher mobility of the grafted PDMAEMA chains in water as compared to the dry state. As shown in Figure 9b, the SPR band positions of PDMAEMA-AuNP nanoassemblies have been found nearly reversible with the modulation of pH for five cycles. Figure 9c compares the SPR band positions of PDMAEMA-AuNP nanoassemblies with the variation in surrounding media and thickness. We observe approximately linear increases in extent of the shift in SPR band position of the grafted PDMAEMA-AuNP layer upon increasing thickness to 353 nm. The extent of the shift in SPR band position reached a plateau, indicating that AuNPs do not penetrate significantly into the brush layer owing to the steric hindrance. It is worth mentioning here that the apparent shift of 11 nm in the absorption band position of the PDMAEMA-AuNP nanoassemblies on the polymer brushes having 432 nm of thickness. It is needless to mention that the extent of the shift in SPR band position manifests the sensitivity of the nanosensors.

One-Dimensional Periodic Relief Grating of PDMAEMA-AuNPs Nanoassemblies. The final step in our strategy was the surface-immobilization of AuNPs onto a patterned PDMAEMA brushes.[52] As shown in Figure 1, the line array in the proposed method were made with e-beam lithography and OPT. We used lithography processes with positive photoresists to fabricate trenches having a 400 nm resolution. Figure 10a displays an AFM image of a trench array, patterned using e-beam lithography, possessing a resolution of 400 nm on the Si wafer. The PDMAEMA brushes were grafted onto the 400 nm resolution trenches through ATRP. Figure 10b reveals that the polymer brushes grafted for 24 h on the Si surface existed as distinctive overlayers. Height of line pattern of the grafted polymer brushes from the trenches is ca. 284 nm, less than 432 nm of thickness, because of the less grafting site on the trench surface.[34] Figure 10c displays an SEM image of a 400 nm resolution OPRG of PDMAEMA brushes, patterned using e-beam lithography over a large area on the Si wafer. We observe

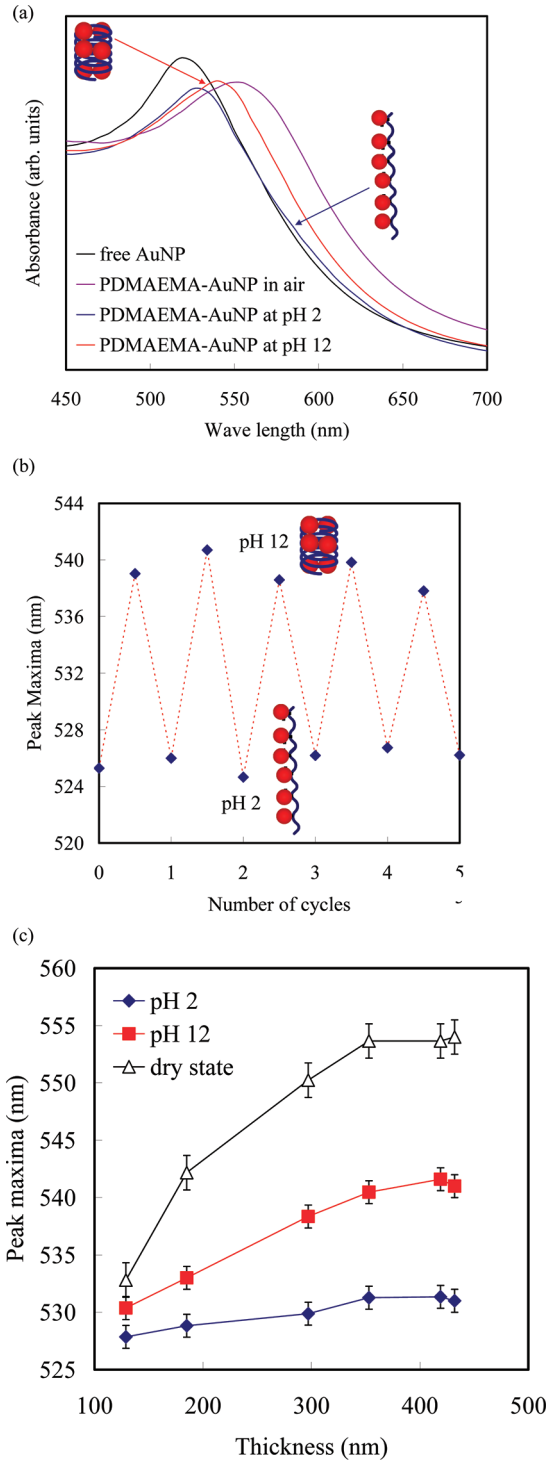

Figure 9. (a) UV−vis spectra of free AuNPs and PDMAEMA-AuNP nanoassemblies taken in air and aqueous media. (b) SPR band positions of AuNPs of the PDMAEMA-AuNP nanoassemblies at pH 2 and 12. (c) Variation in the position of the SPR peak of PDMAEMA-AuNP nanoassemblies with the change in surrounding media from air to water and pH of aqueous media.

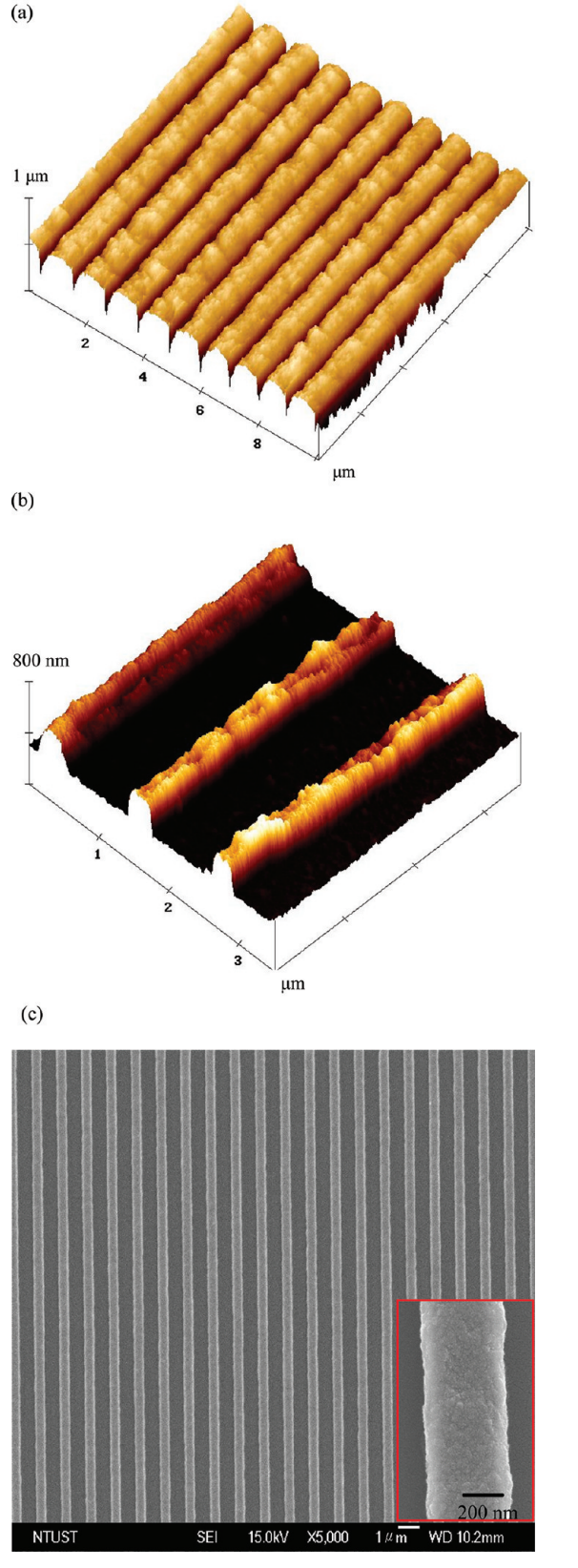

Figure 10. (a) AFM height image (10 × 10 μm) of trench array with a 400 nm resolution obtained by electron beam lithography and (b) OPRG of PDMAEMA brushes grafted from 400 nm resolution trenches. (c) SEM image of b over a large area.

regular line array of the polymer brushes after incubation into toluene overnight. High magnification inside the red line frame in Figure 10c reveals coil-like structure possessing 10−20 nm diameter inside the line array of the polymer brushes.

Images a and b in Figure 11 illustrate topographic SEM images of immobilization of AuNPs on patterned PDMAEMA brushes, grafted for 2 and 24 h, respectively. One can observe that the morphology of the PDMAEMA-AuNP nanoassemblies

dx.doi.org/10.1021/am201632e | ACS Appl. Mater. Interfaces 2012, 4, 1935−1947

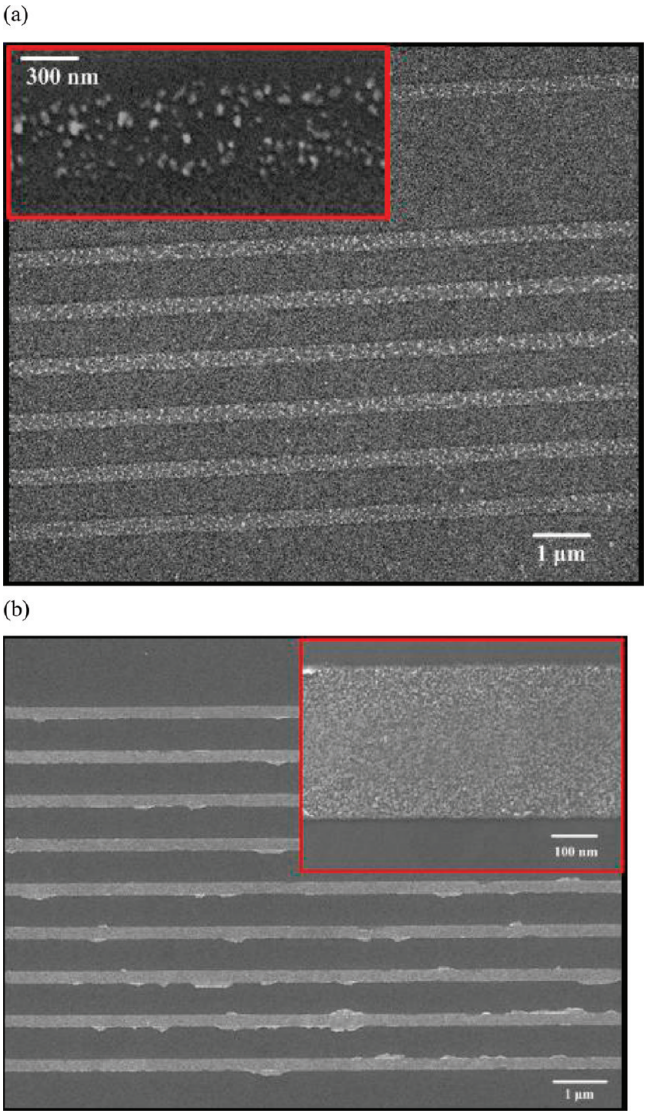

Figure 11. Topographic SEM image of AuNP immobilization on OPRG of PDMAEMA brushes grafted for (a) 2 and (b) 24 h.

in distinctive overlayer has turned from dense (without patterning) to thin one (with patterning). Such thin polymer brushes clustered rapidly with AuNPs as a coil-like structure in distinctive overlayer, indicating that the AuNPs are immobilized on the all part of the shorter polymer brushes to generate apparently AuNP aggregation. We observe unobvious AuNP aggregation on the grafted polymer chains for 24 h, suggesting that the AuNPs dispersed on the longer polymer chains in distinctive overlayer.(Figure 10b) In addition, irregulars of the PDMAEMA-AuNP nanoassemblies appear at the edge of the line array because of collapse of the PDMAEMA-AuNPs nanoassemblies in dry state.

In case of an OPRG, the effective refractive indices for TM and TE polarization are perpendicular and parallel to the line array of the PDMAEMA brushes, respectively. We used the refractive indices of PDEAEMA thin film and Au thin film at 633 nm is reported to be 1.513 and 0.179 as a standard value to measure the refractive index of PDEAEMA-AuNPs thin film by ellipsometry. Figure 12 presents the pH-dependence of the flat PDMAEMA-AuNPs and its OPRG with various thicknesses in terms of refractive indices for TM and TE polarization. Inserted

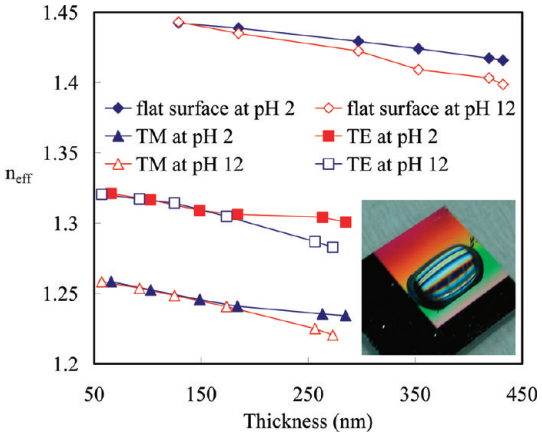

Figure 12. pH-dependence of the flat PDMAEMA-AuNP nanoassemblies and its OPRG in terms of refractive indices for TM and TE polarization with various thicknesses. Insert is the photographic image of WCA along TM and TE directions on OPRG of the PDMAEMA brushes with 284 nm thickness after aqueous solution treatment at pH 2.

photographic image of the PDMAEMA-AuNP OPRG possessing 284 nm thickness after aqueous solution treatment at pH 2 reveals water contact angle (WCA) along TM and TE directions. In the process described above, pH treatment of the PDMAEMA-AuNP grating leads to a reversible conformational changes. This effective enhancing and weakening of OPRG is driven by changes in the degree of immobilization of the AuNPs on PDMAEMA brushes for a pH-responsive switching. Such films possess potential for pH-responsive optical and sensor applications.[53,54] In general, OPRG structure suitable for use as antireflection coatings are created when the acidic solution in this process is in the pH range of 2−6. To confirm the conformational changes of PDMAEMA brush OPRG under various pH treatments, the filling factors (f_{TM} and f_{TE}) of the binary grating was calculated from the refractive indices for TM and TE polarization by eqs 4 and 5, respectively. The pH-dependence of filling factors including f_{TM}, f_{TE}, and their average value f_a of the binary grating are in the range of 0.6−0.7 calculated by eqs 4 and 5. These filling factors exhibited pH-dependent behavior from 2 to 12, verifying the pH-responsive OPRG on the surface. These observations indicate that fabricated nanosensors can be used to sense the nature of the surrounding media such as in microfluidic devices from dry to the wet state and vice versa, as well as pH in aqueous media.

CONCLUSIONS

We have used a "grafting from" system with ATRP to prepare well-defined PDMAEMA brushes on Si wafers. It provides patterned polymeric thin films as OPRG that approach the nanoscale. We establish the ability of the PDMAEMA chains to function as "tentacles" to the immobilization of AuNPs onto the macroscopic surfaces by exploiting the pH-responsive polymer brushes as adhesion promoters. Resulting PDMAEMA-AuNP nanoassemblies and its binary grating have been used for the fabrication of pH nanosensors by exploiting the pH induced swelling−deswelling of polymer brushes and tunable optical properties of PDMAEMA-AuNP nanoassemblies. In addition to demonstrated sensing application, we believe that immobilized NPs can offer the large surface area as compared to the bulk ones. The employed approach is versatile in nature

and can be applied to modify various macroscopic surfaces via immobilization of different types of NPs. One can exploit the same methodology in biological applications for reversible and pH-induced switching of bioactive agents by modifying the surfaces of the interests with PDMAEMA brushes.

AUTHOR INFORMATION

Corresponding Author

*Tel.: +886-2-27376523. Fax: +886-2-27376544. E-mail: jkchen@mail.ntust.edu.tw.

Notes

The authors declare no competing financial interest.

ACKNOWLEDGMENTS

We thank the National Nano Device Laboratory for its financial support of the electron beam lithography system, and the National Science Council of the Republic of China for financially supporting this research, Project 98-2221-E-011-006-MY3.

REFERENCES

(1) Burda, C.; Chen, X.; Narayanan, R.; El-Sayed, M. A. *Chem. Rev.* **2005**, *105* (4), 1025−1102.
(2) Chen, J.-K.; Qui, J.-Q. *Colloid Polym. Sci.* **2011**, *289*, 1829−1837.
(3) Yu, A.; Liang, Z.; Cho, J.; Caruso, F. *Nano Lett.* **2003**, *3*, 1203−1207.
(4) Bharathi, S.; Lev, O. *Chem. Commun.* **1997**, *23*, 2303−2304.
(5) Chen, J.; Qui, J.; Fan, S.; Kuo, S.; Ko, F.; Chu, C.; Chang, F. *J. Colloid Interface Sci.* **2012**, *367*, 40−48.
(6) Chan, C. H.; Chen, J. K.; Chang, F. C. *Sens. Actuators, B* **2008**, *13*, 327−332.
(7) Li, D.; Cui, Y.; Wang, K.; He, Q.; Yan, X.; Li, J. *Adv. Funct. Mater.* **2007**, *17*, 3134−3140.
(8) Agrawal, M.; Pich, A.; Gupta, S.; Zafeiropoulos, N. E.; Simon, P.; Stamm, M. *Langmuir* **2008**, *24*, 1013−1018.
(9) He, Q.; Kueller, A.; Schilp, S.; Leisten, F.; Kolb, H.-A.; Grunze, M.; Li, J. *Small* **2007**, *3*, 1860−1865.
(10) Sandanaraj, B. S.; Bayraktar, H.; Krishnamoorthy, K.; Knapp, M. J.; Thayumanavan, S. *Langmuir* **2007**, *23*, 3891−3897.
(11) Gupta, S.; Agrawal, M.; Uhlmann, P.; Simon, F.; Oertel, U.; Stamm, M. *Macromolecules* **2008**, *41*, 8152−8158.
(12) Chen, J.-K.; Zhuang, A. L *Colloid Polym. Sci.* **2011**, *289*, 1283−1294.
(13) Chen, J.-K.; Li, J.-Y. *Appl. Phys. Lett.* **2010**, *97*, 063701.
(14) Ionov, L.; Sapra, S.; Synytska, A.; Rogach, A. L.; Stamm, M.; Diez, S. *Adv. Mater.* **2006**, *18*, 1453−1457.
(15) Chen, J. K.; Chan, C. H.; Chang, F. C. *App. Phys. Lett.* **2008**, *92*, 053108.
(16) He, Q.; Kueller, A.; Schilp, S.; Leisten, F.; Kolb, H. A.; Grunze, M.; Li, J. *small* **2007**, *3*, 1860−1865.
(17) Kim, S. O.; Solak, H. H.; Stoykovich, M. P.; Ferrier, N. J.; de Pablo, J. J.; Nealey, P. F. *Nature* **2003**, *424*, 411−414.
(18) Stoykovich, M. P.; Muller, M.; Kim, S. O.; Solak, H. H.; Edwards, E. W.; de Pablo, J. J.; Nealey, P. F. *Science* **2005**, *308*, 1442−1446.
(19) Chai, J.; Wang, D.; Fan, X. N.; Buriak, J. M. *Nat. Nanotechnol.* **2007**, *2*, 500−506.
(20) Yan, B.; Thubagere, A.; Premasiri, W. R.; Ziegler, L. D.; Dal Negro, L.; Reinhard, B. M. *ACS Nano* **2009**, *3* (5), 1190−1202.
(21) Coskun, U. C.; Mebrahtu, H.; Huang, P. B.; Huang, J.; Sebba, D.; Biasco, A.; Makarovski, A.; Lazarides, A.; LaBean, T. H.; Finkelstein, G. *Appl. Phys. Lett.* **2008**, *93*, 12.
(22) Ma, L. C.; Subramanian, R.; Huang, H. W.; Ray, V.; Kim, C. U.; Koh, S. J. *Nano Lett.* **2007**, *7* (2), 439−445.
(23) Chen, J.-K.; Li, J.-Y. *Sens. Actuators, B* **2010**, *150*, 314−320.
(24) Chen, J.-K.; Bai, B.-J.; Chang, F.-C. *Appl. Phys. Lett.* **2011**, *99*, 013701.
(25) He, Q.; Tian, Y.; Küller, A.; Grunze, M.; Gölzhäuser, A.; Li, J. *J. Nanosci. Nanotechnol.* **2006**, *6*, 1838−1841.
(26) Chen, J.-K.; Hsieh, C.-Y.; Huang, C.-F.; Li, P.-M. *J. Colloid Interface Sci.* **2009**, *338*, 428−434.
(27) Chen, J.-K.; Chen, Z.-Y.; Lin, H.-C.; Hong, P.-D.; Chang, F.-C. *ACS Appl. Mater. Interfaces* **2009**, *1* (7), 1525−1532.
(28) Ji, S. X.; Liu, C. C.; Liu, G. L.; Nealey, P. F. *ACS Nano* **2010**, *4* (2), 599−609.
(29) Barbey, R.; Lavanant, L.; Paripovic, D.; Schüwer, N.; Sugnaux, C.; Tugulu, S.; Klok, H.-A. *Chem. Rev.* **2009**, *109*, 5437−5527.
(30) Chen, J. K.; Zhuang, A.-L. *J. Phys. Chem. C* **2010**, *114*, 11801−11809.
(31) Paik, M. Y.; Xu, Y.; Rastogi, A.; Tanaka, M.; Yi, Y.; Ober, C. K. *Nano Lett.* **2010**, *10*, 3873−3879.
(32) Jhon, Y. K.; Arifuzzaman, S.; Özç-am, A.; Kiserow, D. J.; Genzer, J. *Langmuir* **2012**, *28*, 872−882.
(33) Kim, B.; Gao, H.; Argun, A. A.; Matyjaszewski, K.; Hammond, P. T. *Macromolecules* **2009**, *42*, 368−375.
(34) Chen, T.-Y.; Chen, J.-K. *Colloid Polym. Sci.* **2011**, *289*, 433−445.
(35) Stoykovich, M. P.; Müller, M.; Kim, S. O.; Solak, H. H.; Edwards, E. W.; de Pablo, J. J.; Nealey, P. F. *Science* **2005**, *308*, 1442−1446.
(36) Yao, Z. L.; Tam, K. C. *Langmuir* **2011**, *27*, 6668−6673.
(37) Carlo, D. D.; Jeong, K.; Lee, L. P. *Lab Chip* **2003**, *3*, 287−291.
(38) Minko, S.; Patil, S.; Datsyuk, V.; Simon, F.; Eichhorn, K. J.; Motornov, M.; Usov, D.; Tokarev, I.; Stamm, M. *Langmuir* **2002**, *18*, 289−296.
(39) Kikuta, H; Toyotai, H.; Yui, W. *Optical Review* **2003**, *10*, 63−73.
(40) Chen, J. K.; Chen, T.-Y. *J. Colloid Interface Sci.* **2011**, *355*, 359−367.
(41) Chen, J.-K.; Li, J.-Y. *J. Colloid Interface Sci.* **2011**, *358*, 454−461.
(42) Zdyrko, B.; Klep, V.; Luzinov, I. *Langmuir* **2003**, *19*, 10179−10l87.
(43) Chen, J.-K.; Bai, B.-J. *Sens. Actuators B* **2011**, *160*, 1011−1019.
(44) Brust, M.; Walker, M.; Bethell, D.; Schiffrin, D. J.; Whyman, R. J. *Chem. Soc., Chem. Commun.* **1994**, 801−802.
(45) Gupta, S.; Agrawal, M.; Uhlmann, P.; Simon, F.; Stamm., M. *Chem. Mater.* **2010**, *22*, 504−509.
(46) Ko, S.; Choi, Y.; Hwang, D. J.; Grigoropoulos, C. P.; Poulikakos, D. *Appl. Phys. Lett.* **2006**, *89*, 141126−141128.
(47) Alivisatos, A. P. *J. Phys. Chem.* **1996**, *100*, 13226−13239.
(48) Elghanian, R.; Storhoff, J. J.; Mucic, R. C.; Letsinger, R. L.; Mirkin, C. A. *Science* **1997**, *277*, 1078.
(49) Storhoff, J. J.; Lazarides, A. A.; Mucic, R. C.; Mirkin, C. A.; Letsinger, R. L.; Schatz, G. C. *J. Am. Chem. Soc.* **2000**, *122*, 4640−4650.
(50) Nath, N.; Chilkoti, A. *J. Am. Chem. Soc.* **2001**, *123*, 8197−8202.
(51) Takeuchi, Y.; Ida, T.; Kimura, K. *Surf. Rev. Lett.* **1996**, *3*, 1205−1208.
(52) Chen, J. K.; Hsieh, C. Y.; Huang, C. F.; Li, P. M.; Kuo, S. W.; Chang, F. C. *Macromolecules* **2008**, *41*, 8729−8736.
(53) Hiller, J.; Mendelsohn, J. D.; Rubner, M. F. *Nat. Mater.* **2002**, *1*, 59−63.
(54) Päivänranta, B.; Sahoo, P. K.; Tocce, E.; Auzelyte, V.; Ekinci, Y.; Solak, H. H.; Liu, C.; Stuen, K. O.; Nealey, P. F.; David, C. *ACS Nano* **2011**, *5*, 1860−1864.